Spatial, single cell profiling of lung SARS-CoV-2

Chin Wee Tan[1], Ning Liu[1], James Monkman[2], Tony Blick[2], Emily Killingbeck[3], Youngmi Kim[3], Dharmesh Bhuva[1], Jinjin Chen[1], Malvika Kharbanda[1], Kristen Feher[1], Belinda Phipson[1], Michael Leon[3], Sarah Murphy[3], Nathan Schurman[3], Mark Gregory[3], Kirsty Short[2], Michael Rhodes[3], Gabrielle Belz[2], Fernando Guimaraes[2], Melissa J Davis[1], **Arutha Kulasinghe*[2]**

*[1] The Walter and Eliza Hall Institute of Medical Research, Parkville, Melbourne, Victoria, Australia, [2] The University of Queensland, Brisbane, Queensland, Australia, [3] Nanostring Technologies, Seattle, WA 98109 *arutha.kulasinghe@uq.edu.au @aruthak*

Study Summary

SARS-CoV-2 has caused a broad spectrum of diseases, ranging from asymptomatic to Acute Respiratory Distress Syndrome (ARDS). Little is known about the host tissue and cellular responses associated with COVID-19 infection, symptoms, and disease severity.

Here, we use the ***Nanostring GeoMX Digital Spatial Profiler (DSP)*** and ***CosMX Spatial Molecular Imager*** **(SMI)** technology to determine tissue signatures, and spatially resolved quantitative single-cell transcriptomic changes driven by SARS-CoV-2 infection. Rapid autopsy COVID-19 lung samples were collected across two independent cohorts of patients, and tissue microarrays (TMAs) were prepared. For GeoMx, n=10 COVID-19, n=10 pH1N1 and n=5 normal control tissues were compared. For CosMx, n=19 COVID-19 cores in technical replicates, and n=20 normal control tissues were compared.

Analysis of the GeoMx data revealed tissue signatures associated with SARS-CoV-2 infection. SMI enabled cell typing and mapping of complex cell populations while preserving spatial context and highlighted differential cell types distribution in the lungs of COVID-19 patients compared to non-infected controls.

Methods

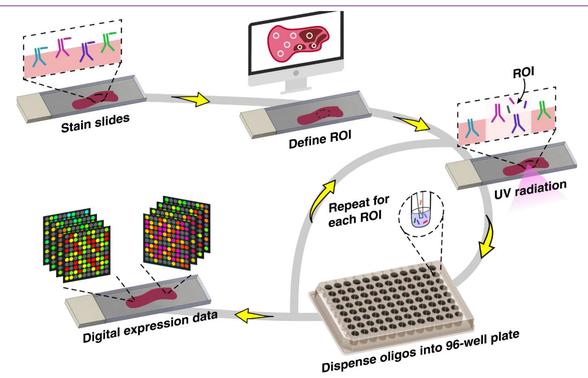

Figure 1. Nanostring GeoMx Digital Spatial Profiler (DSP) workflow.

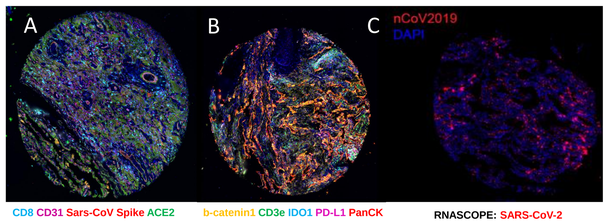

Figure 2. Multiplex-IF imaging of tissue microarray cores stained for (A) CD8, CD31, SARS-CoV-2 virus, ACE2 (B) b-catenin, CD3, IDO1, PDL1, PanCK (C) RNAscope SARS-CoV-2 virus.

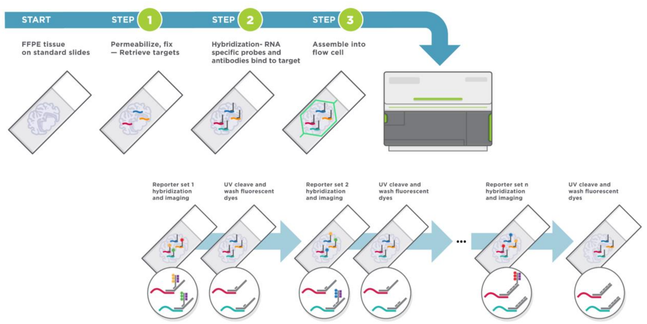

Figure 3. Nanostring CosMx workflow (1000 transcripts/cell assay) ~ 50,000 cells/field of view (FOV) captured across the 1mm cores

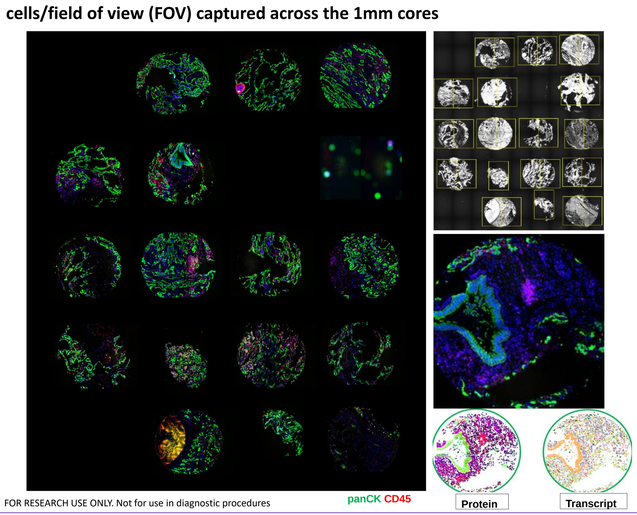

GeoMx® Results

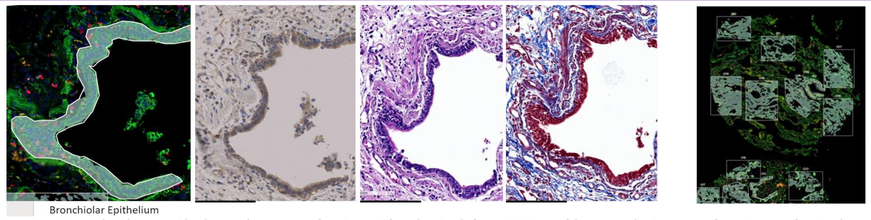

Figure 4. Bronchiolar epithelium 'region of interest' selected for DSP profiling and staining for Mason's Trichrome, H&E. (B) RNAscope for 'SARS-CoV-2' virus (red) in a core of a TMA. Similarly, Type 2 pneumocytes (T2 Pneu), macrophages (macro), hyaline membranes (hyaline).

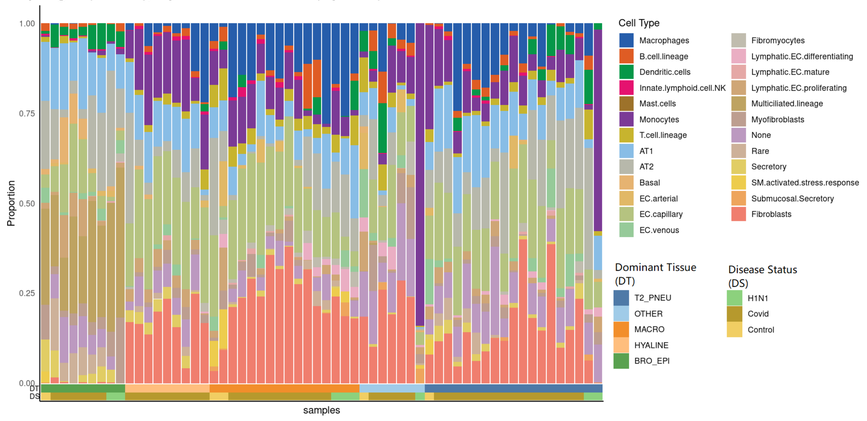

Figure 5. Cell deconvolution across COVID-19, pH1N1 and control cores

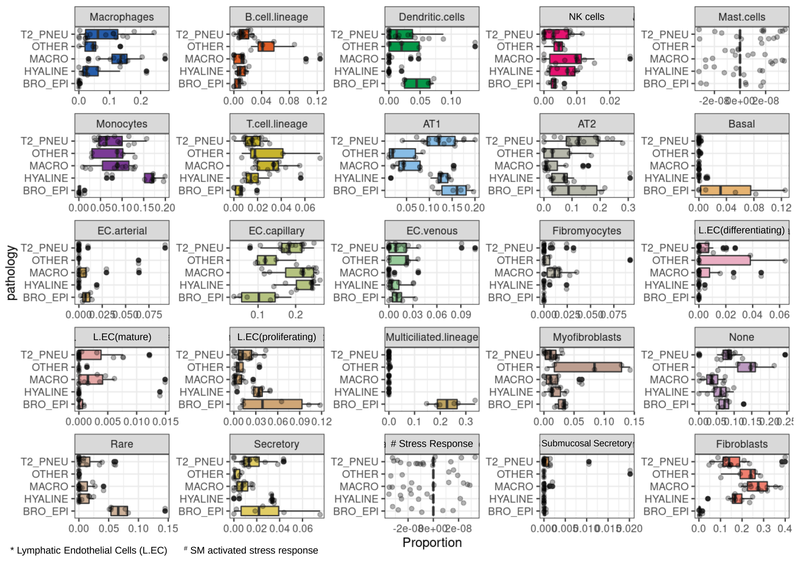

Figure 6. Proportions of cells contributing to the cell type in the pathologically defined regions of the COVID19 samples.

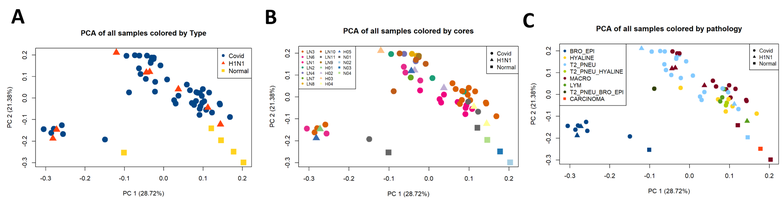

Figure 7. Principle component analysis of the transcriptomics data by (A) disease annotation (COVID-19, pH1N1, Normal control tissues) (B) ROIs selected across patient samples (C) Overlay of the pathology assessment for the majority cell type

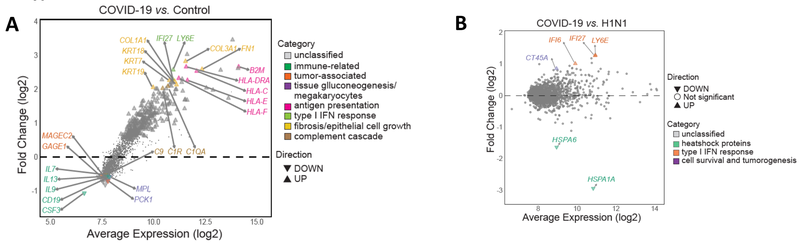

Figure 8. COVID-19 infection drives pro-inflammatory response and suppresses immune cell effector and regeneration. Distribution of differentially expressed genes as a function of the average transcript expression and fold change (log2) identified in (A) COVID-19 samples vs uninfected control and (B) COVID-19 samples vs pH1N1 samples.

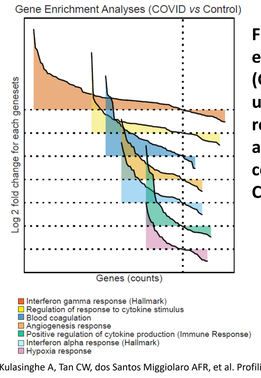

Figure 8. Gene set enrichment analyses (GSEA) reveals upregulated cytokine responses with accompanying coagulopathies in COVID-19 infection.

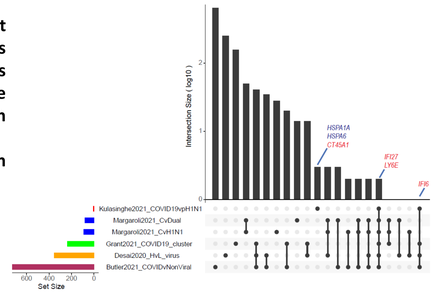

Figure 9. Comparison of COVID specific gene sets identified across 5 different studies.

Kulasinghe A, Tan CW, dos Santos Miggiolaro AFR, et al. Profiling of lung SARS-CoV-2 and influenza virus infection dissects virus-specific host responses and gene signatures. European Respiratory Journal. 2021:2101881

CosMx™ Results

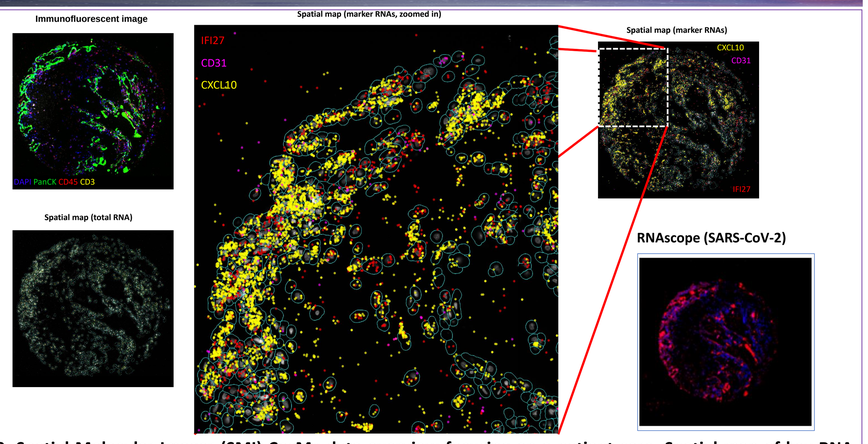

Figure 9. Spatial Molecular Imager (SMI) CosMx data overview focusing on a patient core. Spatial map of key RNA transcripts amongst the cellular neighbourhoods alongside morphological markers and RNAscope overlays for SARS-CoV-2.

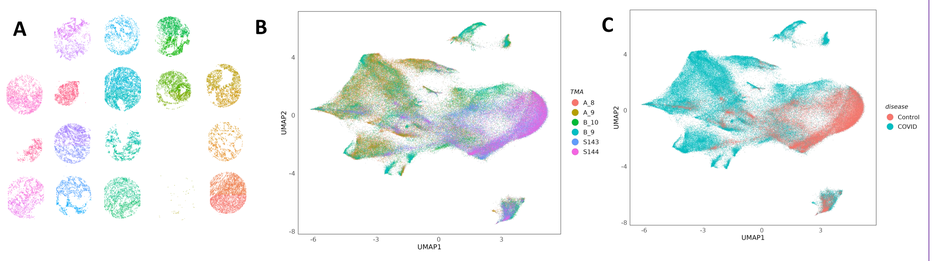

Figure 10. Visualisation of single cells information. (A) Mapping of each cell spatial positions on the tissue cores. UMAPs stratifying by (B) slides and (C) disease status.

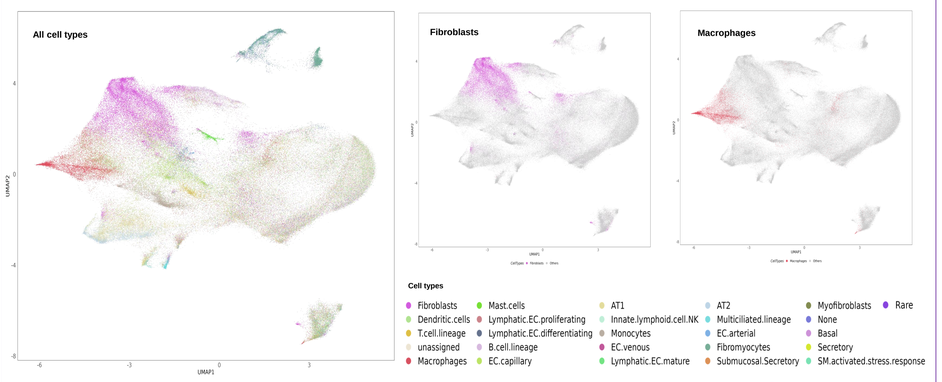

Figure 11. Cell type annotation using an ensemble approach based on 5 established methods. Cell types were identified as the common cell type in ≥ 2 methods and labeled in the UMAP. Fibroblast and macrophage cells were highlighted in the corresponding UMAPs.
(right) spatial location and distributions of the identified cell types in a specific core.

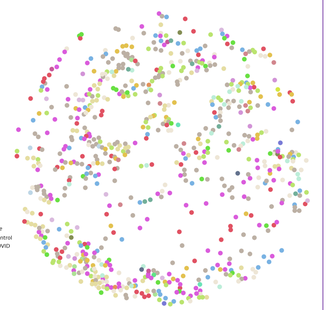

Figure 12. PCA for selected cell types. PCA for either (left) fibroblasts or (right) macrophages pseudo-bulked samples.

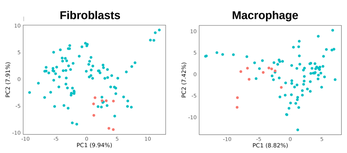

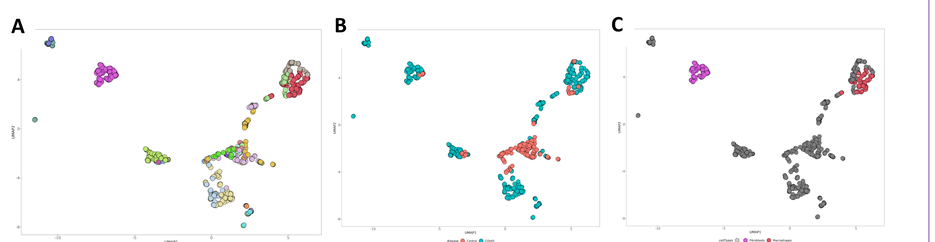

Figure 13. UMAP of pseudo-bulked samples stratified by (A) all cell types, (B) disease status and (C) fibroblast and macrophages.

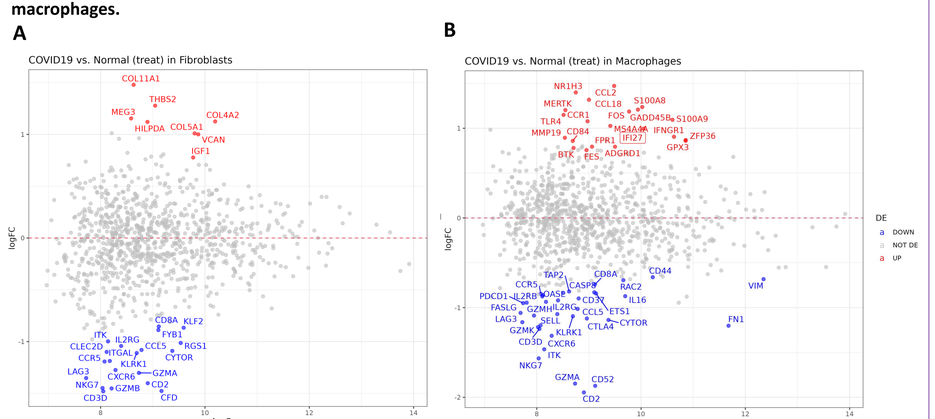

Figure 14. Differential Expression between COVID19 vs Control Samples. Log fold change vs average expression plots for COVID19 vs Control pseudo-samples for either (A) fibroblasts or (B) macrophages cells.